A Solution to the Pioneer Anomalous Annual and Diurnal Residuals

Eduardo D. Greaves[1], Carlos Bracho[2], Stephan Gift[3], and An Michel Rodriguez[4]

[1]Universidad Simón Bolívar. Apartado 89000, Caracas, Venezuela. E-mail: egreaves20002000@yahoo.com
[2]Facultad de Ingeniería, Universidad Central de Venezuela, Caracas, Venezuela. E-mail: bracho_carlos@hotmail.com
[3]Department of Electrical and Computer Engineering, Faculty of Engineering, The University of the West Indies, St Augustine, Trinidad and Tobago, West Indies. E-mail: stephan.gift@sta.uwi.edu
[4]Universidad Simón Bolívar. Apartado 89000, Caracas, Venezuela. E-mail: anmichel.rodriguez@gmail.com

NASA's reported Pioneer 10 and 11 anomalous annual and diurnal Doppler residuals remain largely unexplained. We show they are due to the use of an invariant value of the speed of light c in the Doppler formula. The addition of the orbital speed of the Earth ($\sim 30\,\mathrm{km/s}$) and the Earth's tangential rotational speed ($\sim 0.4\,\mathrm{km/s}$) to the speed of light in the Doppler formula, as [18] has shown to be the velocity addition to be used, adequately fit the measured annual and diurnal Pioneer residuals. This experimentally confirms that the galilean addition of relative velocities to the speed of light satisfactorily explains the measured residuals. The newly reported values from independent analyses of the data, of the reputably constant anomalous Pioneer acceleration as a function of time, or distance from the Sun, are calculated. The values obtained, without any adjustable parameters, coincide within a percent with the experimentally measured values and are consistent with the change of the speed of light due to a decrease in the gravitational energy density with distance from the Sun as postulated by the Céspedes-Curé hypothesis. This result implies reassessment of all astronomical velocity measurements based on the Doppler Effect that have led to current cosmological theories: the Hubble constant, the expansion of the universe, the flat rotation curve of galaxies and the extreme values of the redshifts of very far away galaxies.

1 Introduction

Most of the physics related to astronomy and cosmology had been in the past based on passive astronomical observation of the measurements used to derive the theories. This is the case for Isaac Newton who derived his universal theory of gravitation from Johannes Kepler, who in turn used his own and the detailed observations of Tycho Brahe to develop his laws of planetary motion. Likewise, observations of the total Sun eclipse of 1919 by the team led by Arthur Stanley Eddington provided the first evidence in support of Einstein's General Theory of Relativity

In recent times, observational instruments have become increasingly powerful expanding visual telescopes to other ranges of the electromagnetic spectrum such as to the lower region, and to the higher regions with the radio telescopes and the x-ray and gamma ray observational satellites. These instruments have expanded our vision to ever further regions of the past history of the Universe. Moreover, with the advent of space exploration with Earth satellites and the launch of deep space probes, astronomy and cosmology now routinely utilize experimental probes to examine, refine, support or create physical theories of the cosmos. With the introduction of digital processing, computing power, extremely precise timing and the development of very high frequency electronics, accurate observations have increased to previously unforeseen ranges.

One such case is the measurement by the space agencies of extremely small phenomena that have shown minute but significant deviations from the values predicted by accepted physical theories and that have defied for lengths of time satisfactory explanation. Two examples are deviations from the predicted hyperbolic movement of space probes: the Flyby Anomaly [1, 2] and the Pioneer Anomaly [3–5]. In the Flyby Anomaly, the energy assist maneuver about the planets has been shown in several probes to deviate from the expected energy conservation prediction. In this case, speed deviations of mm/s reported are detected with errors of 10^{-2} mm/s on probes moving at speeds of several km/s.

The Pioneer Anomaly measurements of the hyperbolic movement of Pioneer 10 and 11 as well as Ulysses and Galileo have shown a minute acceleration in excess of the expected slowing towards the Sun due to its gravitational attraction. The deviations are of the order of 10^{-8}. The realization of these measurements is an extraordinary accomplishment considering that the probes are located far away in the solar system, moving at velocities in the range of several km/s. The anomalous measurements are reported with an accuracy of $\sigma_{at} = 0.32 \times 10^{-10}\,\mathrm{m/s^2}$ [5].

In addition to the assumed constant anomalous acceleration, Pioneer's Doppler residual measurements have shown annual and diurnal oscillations about the average acceleration with amplitude of about $0.8 \times 10^{-9}\,\mathrm{m/s^2}$ (see Fig. 4). The magnitudes of the diurnal terms are reported to be comparable to those of the annual term. These results have been the subject of considerable discussion in the published literature: Anderson *et al* in 2002 [3, p. 40–43] concluded that they are

not spacecraft-related phenomena nor artifacts of the measuring system but that they are Earth-related phenomena. In particular, the diurnal Doppler residuals exhibit a period that is close to the Earth's sidereal period.

Nieto and Anderson in 2005 [6] reported, in a very clear review, sinusoidal fits to the annual residuals showing similar values for Pioneer 10 and 11 and a phase difference of 173.2 degrees, similar to the angular separation of the two spacecrafts in ecliptic longitude.

There have been other attempts to explain the periodic anomalies. O. Olsen in 2007 [7] stated that unmodeled short-term effects are claimed to be consistent with expected values of radio plasma delay and the electron content of the Sun's Coronal Mass Ejections. Small annual and diurnal terms are considered to be artifacts of the maneuver estimation algorithm and unmodeled effects.

A. Ghosh in 2007 [8] attempted to explain these fluctuating components as due to the motions of the Earth and excess redshifts of the signal caused by velocity dependent inertial induction. He appears to be able to explain the annual and diurnal fluctuations in the anomalous acceleration of Pioneer 10.

Levi *et al* in 2009 [9] performed a data analysis independent of that of Anderson *et al* (2002), using the same data and confirming the existence of a secular anomaly. This anomaly has amplitude of about 0.8×10^{-9} m/s^2 that is compatible with that reported by Anderson *et al*. Their fit to the diurnal residuals showed the presence of significant periodic terms with the periods measured with respect to a day of 86 400 s. They reported, very accurately, periodic terms consistent with variations of one sidereal day, half a sidereal day, and half a year.

A later report on the Pioneer Anomaly by Turyshev and Toth in 2010 [5, Sec. 5.5.4, p. 86] acknowledged the presence of these oscillatory Doppler residuals ascribing them to "a mismodeling of the orbital inclination of the spacecraft to the ecliptic plane". However, in Section "7.2 Unresolved questions", it is mentioned that "Even after a best fit analysis is completed, the resulting residual is not completely random: both annual and diurnal variations are clearly visible. Is it possible to pinpoint the source of these variations?".

The current opinion (2021) that the Pioneer Anomaly was resolved as a thermal effect rests on a paper by S. G. Turyshev *et al* (2012) [10] which does a complex parametrized model for the thermal recoil force of the Pioneer spacecraft with several adjustable parameters. In particular the two adjustable parameters of Eq. (1) on page 2 predict the anomaly. However, any other parameters would negate the thermal origin of the anomaly.

Other reports that also support the thermal origin are: Rievers and Lammerzahl (2011) [12] and Francisco *et al* (2012) [13]. However, the detailed paper about the Pioneer Anomaly (55 pages of Phys. Rev. by J. D. Anderson *et al* (2002) [3]) clearly argues (see Sections VIII.B, C and D, pp. 32–35) that thermal recoil cannot account for the anomaly. Additionally, an anomaly similar to the Pioneer spacecraft was detected in Galileo spacecraft (see Section V C, p. 21) [3] and in the Ulysses spacecraft (see Section V D, p. 21) [3]. Both spacecrafts have completely different geometries and the thermal recoil theory is not applicable to them. Furthermore, the anomalous acceleration is reported to change value, decreasing rapidly and then increasing, (see discussions below, Sections 2.2 and 5.3 and references therein) during the spacecrafts' Jupiter and Saturn encounters. These reported changes of the anomaly as well as the harmonic annual and diurnal variations clearly cannot be explained by a thermal recoil theory.

More recently, L. Bilbao in 2016 [11], making use of the Vibrating Rays Theory [14], claims that relating the velocity of light and the corresponding Doppler effect with the velocity of the source at the time of detection, instead of the time of emission, it is possible to explain quantitatively and qualitatively the spacecraft anomalies. Values calculated for the annual residual approximately coincide with reported measurements for Pioneer 10 at 40 AU, $\Delta f \approx 14$ mHz and for Pioneer 11 at 69 AU, $\Delta f \approx 4.8$ mHz [11, p 310]. However, on the same arguments, the theory would predict values 5 or 6 orders of magnitude smaller than reported for the diurnal Doppler residuals measurements.

In this paper, an explanation of the constant term of the Pioneer Anomaly by Greaves in 2008 [4, 15] is reviewed with updated results and a new explanation of the oscillatory nature of the annual and diurnal Doppler residuals is presented. Both explanations are in agreement with the galilean velocity addition. The harmonic fluctuations make use of the results of analysis by Gift in 2010 of the Doppler Effect [16], in 2014 [17] and in 2017 of the Global Positioning System (GPS) [18].

2 Pioneer anomaly reported values

In order to compare the theoretical predictions with the reported values, in this section we review the literature with special emphasis on the particular phenomena pertinent to the theory presented about the anomalous acceleration values. In the light of the results below that imply different values depending on distances from the Sun and hence at the various measurement times, we do not find it surprising that a variety of values are reported.

The Pioneer Anomaly is the result of a complicated modeling procedure involving the gravitational physics predicting the probe trajectory, newtonian and relativistic, as well as a cornucopia of other phenomena such as solar radiation pressure and electromagnetic line of sight effects. The result of the modeling is compared to the measured Doppler signals received and processed by the Deep Space Network (DSN) by means of mathematical least squares fitting procedures. While there may be several possible onboard causes of anomalous results such as gas leaks or the now popular

effect of asymmetric thermal radiation pressure, the different programs that have been developed generally agree on the existence of an anomaly.

We start by citing the anomalous measurements of the Galileo and Ulysses spacecrafts given by Anderson *et al* (2002) [3, p. 22, Eq. (18)]. Unfortunately, not many details are given for these anomalous measurements.

2.1 Galileo

The reported JPL values of Aerospace's analysis for the dates 2 December 1992 to 24 March 1993 give an anomalous acceleration of $a_{P(G)} = (8 \pm 3) \times 10^{-8}\,\mathrm{cm/s^2}$.

Galileo performed a second flyby of Earth at 303.1 km height at 15:09:25 UTC on 8 December 1992, adding 13,320 km/h to its cumulative speed on the way to Jupiter. Hence the reported Galileo $a_{P(G)}$ is just on or after the Earth flyby at approx. 1 AU distance from the Sun, and under full Earth and Sun gravitational acceleration field [19].

2.2 Ulysses

The JPL analysis gives $a_{P(U)} = (12 \pm 3) \times 10^{-8}\,\mathrm{cm/s^2}$. The data is from 30 March 1992 to 11 August 1994. Ulysses arrived at Jupiter on 8 February 1992 for a flyby maneuver that increased its inclination to the ecliptic by 80.2 degrees southward, away from the ecliptic plane entering an orbit around the Sun. The orbital period is approximately six years. The Sun's gravitational acceleration at the Jupiter orbit is $g_S = 2.1 \times 10^{-4}\,\mathrm{m/s^2}$, four orders of magnitude smaller than Jupiter's $g_j = 0.227\,\mathrm{m/s^2}$ gravitational acceleration at the nearest point in the flyby (4.09×10^8 m). The flyby was engineered to bring Ulysses into a Sun elliptical orbit, so that after the flyby Ulysses began movement towards the Sun with the resulting gravitational acceleration $\vec{g}_U = \vec{g}_S + \vec{g}_j$ pointing generally towards Jupiter for some time until the distance to the Sun was ≈ 5 AU. Thereafter Ulysses acceleration $\vec{g}_U$ points generally towards the Sun. Aerospace's analysis using CHASMP reports no numerical value due to measurement difficulties. However, it is stated: "The measured anomalies randomly changes sign and magnitude. The values go up to about an order of magnitude larger than a_P" [3, p 22]. This measurement and remark of Ulysses' anomalous acceleration is when the spacecraft was under Jupiter gravitational attraction just after the flyby and hence with net gravitational acceleration towards Jupiter and sometime later towards the Sun.

2.3 Pioneer 10 and 11

Table 1 of Anderson *et al* (2002) [3, p 23] reproduced below, with its original caption, gives an indication of the variability of reported values. The original data analyzed is for the following periods:

Pioneer 10: 11 years time interval (3 January 1987 to 22 July 1998), covers a heliocentric distance interval from 40 AU to 70.5 AU.

Program/Estimation method	Pio 10 (I)	Pio 10 (II)	Pio 10 (III)	Pio 11
Sigma, WLS, no solar corona model	8.02 ± 0.01	8.65 ± 0.01	7.83 ± 0.01	8.46 ± 0.04
Sigma, WLS, with solar corona model	8.00 ± 0.01	8.66 ± 0.01	7.84 ± 0.01	8.44 ± 0.04
Sigma, BSF, 1-day batch, with solar corona model	7.82 ± 0.29	8.16 ± 0.40	7.59 ± 0.22	8.49 ± 0.33
CHASMP, WLS, no solar corona model	8.25 ± 0.02	8.86 ± 0.02	7.85 ± 0.01	8.71 ± 0.03
CHASMP, WLS, with solar corona model	8.22 ± 0.02	8.89 ± 0.02	7.92 ± 0.01	8.69 ± 0.03
CHASMP, WLS, with corona, weighting, and F10.7	8.25 ± 0.03	8.90 ± 0.03	7.91 ± 0.01	8.91 ± 0.04

Table 1: Determinations of a_P in units of $10^{-8}\mathrm{cm/s^2}$ from the three time intervals of Pioneer 10 data and from Pioneer 11. As described in the text, [our Ref. 3] results from various ODP-Sigma and CHASMP calculations are listed. For ODP-Sigma, "WLS" signifies a weighted least-squares calculation, which was used with i) no solar corona model and ii) the 'Cassini' solar corona model. Also for ODP/Sigma, "BSF" signifies a batch-sequential filter calculation, which was done with iii) the 'Cassini' solar corona model. Further (see Section IX C), a 1-day batch-sequential estimation for the entire data interval of 11.5 years for Pioneer 10 yielded a result $a_P = (7.77 \pm 0.16) \times 10^{-8}\,\mathrm{cm/s^2}$. The CHASMP calculations were all WLS. These calculations were done with i) no solar corona model, ii) the 'Cassini' solar corona model, iii) the 'Cassini' solar corona model with corona data weighting and F10.7 time variation calibration. Note that the errors given are only formal calculational errors. The much larger deviations of the results from each other indicate the sizes of the systematics that are involved. (Acronyms are: ODP - JPL's Orbit Determination Program; CHASMP - Aerospace Corporation's Compact High Accuracy Satellite Motion Program.)

Pioneer 11: data of 3 years (5 January 1987 to 1 October 1990), covers a heliocentric distance interval much closer to the Sun, from 22.42 to 31.7 AU.

Additionally, Anderson *et al* (2002) [3, on p. 27] quote: "For Pioneer 10, two different analysis programs: Sigma and CHASMP (*measurements*) are similar, $7.82 \times 10^{-8}\,\mathrm{cm/s^2}$ and $7.89 \times 10^{-8}\,\mathrm{cm/s^2}$, the weighted average of these two to yield $a_{Pio10} = (7.84 \pm 0.01) \times 10^{-8}\,\mathrm{cm/s^2}$ (experimental).

"For Pioneer 11, we only have the one 3 3/4 year data arc. The weighted average of the two programs' no corona results is $(8.62 \pm 0.02) \times 10^{-8}\,\mathrm{cm/s^2}$."

2.3.1 Information of planetary encounters

The Pioneer 10 original data spans heliocentric distance interval from 40 AU to 70.5 AU, as mentioned above. Hence it does not include the Jupiter flyby at 5.2027 AU on 1974.

Pioneer 11's original data covers a heliocentric distance interval from 5.80 to 29.50 AU. It includes just after the Jupiter flyby at 5.2027 AU and the Saturn encounter at 9.546 AU on 1979. Also near encounter with Uranus at 19.2 AU on approx. 1986 and with Neptune at 30.09 AU on approx. 1990. Moreover, a report in 2005 of Nieto and Anderson [6] pro-

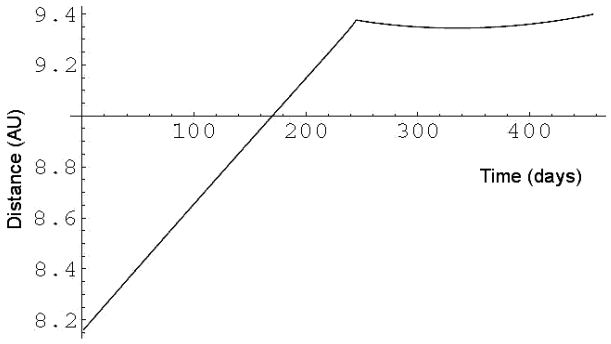

Fig. 1: "A plot of Pioneer 11's distance from the Sun (in AU) vs time (in days starting with 1 Jan. 1979) near Saturn encounter (on Sept. 1, 1979)" [6, p 14]. *Captions of axes added.*

vides additional insight to the planetary encounters and the harmonic residuals. They report that the initial two points in the Pioneer 11 anomalous acceleration shown in their Figures 4 and 5 (our Fig. 2) were near the distances of Jupiter and Saturn encounters. They provide a figure showing the distance (AU) as a function of time (in days) around the Saturn flyby of Pioneer 11. See Fig. 1 with its original caption.

We find this figure very illuminating as at these times the spacecraft was under the gravitational attraction of Saturn and perhaps also under the influence of its higher space energy density as discussed below.

Regarding the annual residuals, Nieto *et al* [6] mention on p. 14:

> Plots of the anomaly versus time were also made from these data points. These showed, as might be suspected from Figures 4 and 5, [our Fig. 2] a possible annual variation. This observation would be a forerunner of the discussion in Section IX-C of [12], [our Ref. [3]]. Doing fits to the data points, the best estimate of the amplitude of the Pioneer 10 sine wave is $(0.525 \pm 0.155) \times 10^{-8}$ cm/s^2 and that of the Pioneer 11 wave is $(0.498 \pm 0.176) \times 10^{-8}$ cm/s^2 (here with the first three points omitted). The sine waves seem real, with, e.g. a 95 percent probability that the Pioneer 10 amplitude lies between 0.199 and 0.834×10^{-8} cm/s^2. The difference in phase between the Pioneer 10 and Pioneer 11 waves is 173.2 degrees, similar to the angular separation of the two spacecrafts in ecliptic longitude. [This is 204.28 degrees at the present time.]

Useful information is provided in Table II which contains the numerical data for each spacecraft containing the distance, dates, reported anomalous acceleration a_P and the error ΔP. Using this information, we find it helpful to plot the reported dates and distances (see Fig. 3) as this information allows the determination of the distance or dates of reported a_P when the information is not given.

Craft	Distance	Dates	a_P	σ_P
Pioneer 11	5.80	77/270-1	0.69	1.48
(Saturn Encounter)	9.38	79/244		
	9.39	80/66-78	1.56	6.85
	12.16	82/190-1	6.28	1.77
	14.00	83/159	8.05	2.16
	16.83	84/254	8.15	0.75
	18.90	85/207	9.03	0.41
	22.25	86/344-5	8.13	0.69
	23.30	87/135-6	8.98	0.30
	26.60	88/256-7	8.56	0.15
	29.50	89/316-7	8.33	0.30
Pioneer 10	26.36	82/19	8.68	0.50
	28.88	82/347-8	8.88	0.27
	31.64	83/346	8.59	0.32
	34.34	84/338-9	8.43	0.55
	35.58	85/138	7.67	0.23
	37.33	86/6-7	8.43	0.37
	40.59	87/80	7.45	0.46
	43.20	88/68	8.09	0.20
	45.70	89/42-3	8.24	0.20

Table 2: Pioneer 11 and 10 early data points (Distance in AU, Date year/days-of-year, anomaly a_P and error σ_P in units of 10^{-8} cm/s^2 from [6].

Toth and Turyshev in 2007 [20, p. 15] comment results found during the Jupiter–Saturn cruise phase: "Right at the time of the Saturn encounter, however, when the spacecraft passed into an hyperbolic escape orbit, *there was a rapid increase in the anomaly, whereafter it settled into the canonical value*" [our emphasis].

2.3.2 Independent analysis of Pioneer data

There have been several further independent analyses of the original data which were made available since 2002 and are reviewed below.

C. Markwardt (2002) [21] performed an independent analysis of radio Doppler tracking data from the Pioneer 10 spacecraft for the time period 1987–1994. His best-fit value for the acceleration, including corrections for systematic biases and uncertainties, is $(8.60 \pm 1.34) \times 10^{-8}$ cm/s^2, directed towards the Sun.

O. Olsen (2007) [7] does an independent analysis of the Pioneer 10 and 11 data using the HELIOSAT program developed by one of the authors at the University of Oslo. The data used spans the three periods defined by Anderson *et al* (2002) for Pioneer 10: Interval I spans 1 January 1987 to 17 July 17 1990, Interval II spans 17 July 1990 to 12 July 12 1992 and Interval III continues up to 21 July 1998. The anomalous accelerations ($\times 10^{-8}$ cm/s^2) obtained are given in his Table I from which we extract: Pioneer 10: Interval I = 7.85 ± 0.02;

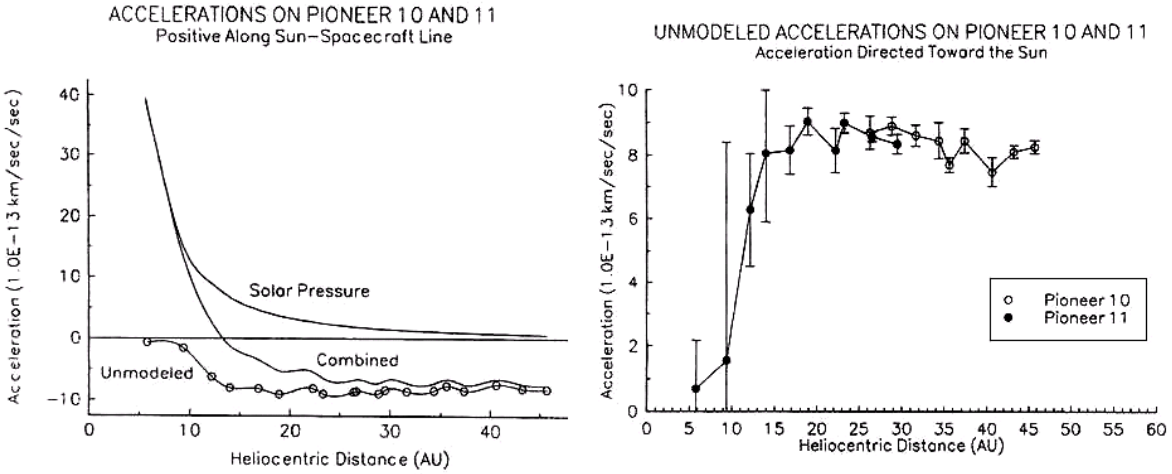

Fig. 2: Left: Accelerations on the Pioneer spacecraft. Right: Anomalous acceleration as a function of distance [3, p. 19].

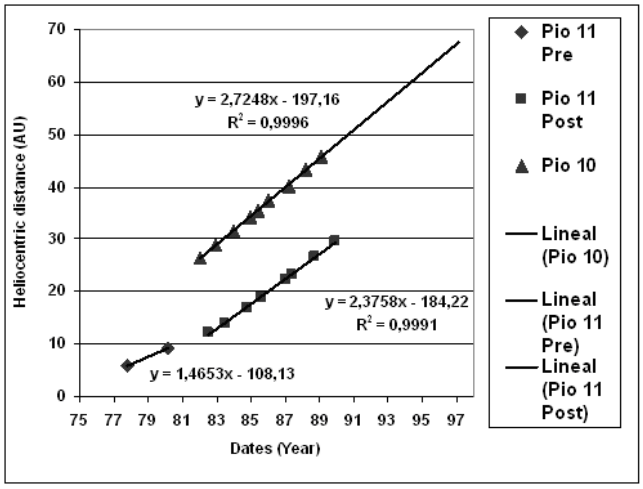

Fig. 3: Heliocentric distance (AU) as a function of dates (year) for Pioneer 10 and 11 positions. Lines are linear fits. For Pioneer 11 pre and post Jupiter flyby. (Data from Table II.)

Interval II = 8.78 ± 0.01; Interval III = 7.75 ± 0.01; Pioneer 11 = 8.10 ± 0.01. From the paper's conclusions: "The unmodeled short term effects are claimed to be consistent with expected values of radio plasma delay and the electron content of Coronal Mass Ejections. Small annual and diurnal terms are ascribed as artifacts of the maneuver estimation algorithm and unmodeled effects acting on the spacecraft or on the radio transmissions."

V. T. Toth does an independent analysis of the orbit of the Pioneer spacecrafts reporting in 2009 [22, p. 18] for Pioneer 10* $a_{P10} = (9.03 \pm 0.86) \times 10^{-8}\,\mathrm{cm/s^2}$ (period 1987 to 1998) and for Pioneer 11 $a_{P11} = (8.21 \pm 1.07) \times 10^{-8}\,\mathrm{cm/s^2}$ (period 1986 to August 1990). Toth also attempted in his analysis to test the extent to which the anomalous acceleration is constant in time. To this end, he implemented the ability to estimate a secondary acceleration, i.e. "jerk" term in the orbital solution.

The results obtained were: for Pioneer 10, $a_{P10} = (10.96 \pm 0.89) \times 10^{-8}\,\mathrm{cm/s^2}$ [3, p. 20], with a variation rate of $da_{P10}/dt = -(0.21 \pm 0.04) \times 10^{-6}\,\mathrm{cm/s^2/year}$ and for Pioneer 11, the result was $a_{P11} = (9.40 \pm 1.12) \times 10^{-8}\,\mathrm{cm/s^2}$, with a variation rate of $da_{P11}/dt = -(0.34 \pm 0.12) \times 10^{-8}\,\mathrm{cm/s^2/year}$. Toth goes on to state: "an anomalous acceleration that is a slowly changing function of time (*decreasing*) cannot be excluded at present" [our italics].

Levi *et al* in 2009 [23] performed a data analysis independent from that of Anderson *et al* (2002) using the same Pioneer 10 data confirming the existence of a secular anomaly with an amplitude of about $8 \times 10^{-8}\,\mathrm{cm/s^2}$ compatible with that reported by Anderson *et al* (2002) and providing additional insight into the phenomenon.

2.4 Annual and diurnal Doppler residuals

The first indication of the oscillatory nature of the Pioneer Anomaly came from an examination of the data in Fig. 2. The observations are addressed in detail in Anderson *et al* (2002) [3, pp. 40-41]. From that report, we show Figs. 4, 5 and 6.

Levi *et al* in 2009 [9], performed an important and illuminating independent analysis of the diurnal periodic terms during a short time span of (we quote): "23 November 1996 to

*Toth and Levi *et al* express all values in SI units. We have converted accelerations to $\mathrm{cm/s^2}$ as used in most Pioneer reports.

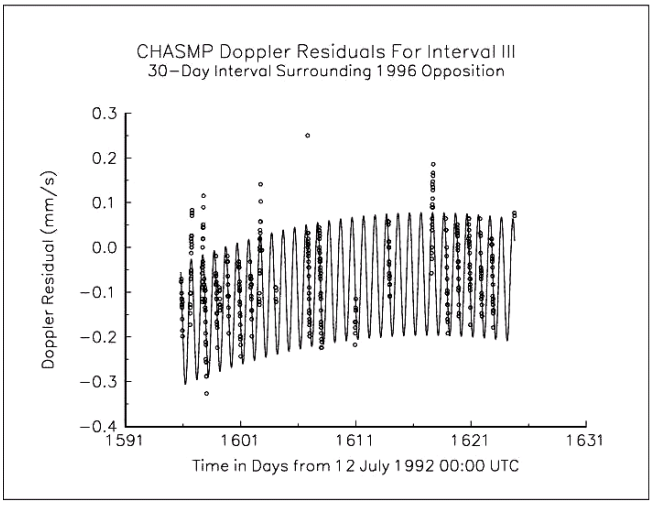

Fig. 4: Diurnal residuals. "CHASMP acceleration residuals from 23 November 1996 to 23 December 1996" [3, Fig. 18, p. 41].

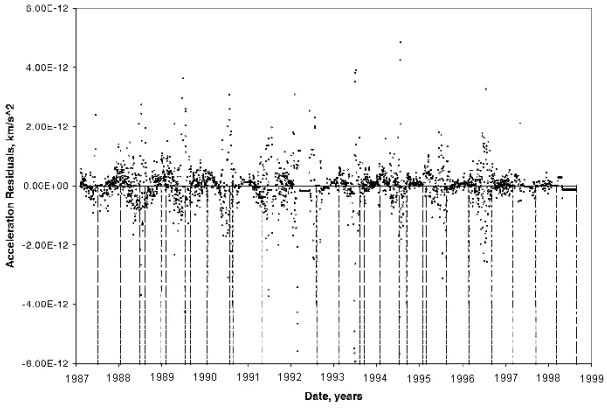

Fig. 5: Annual residuals. "ODP 1-day batch-sequential acceleration residuals using the entire Pioneer 10 data set. Maneuver times are indicated by the vertical dashed lines". [3, Fig. 17, p. 40].

23 December 1996 when Pioneer 10 was on opposition (Sun, Earth and Pioneer 10 aligned in this order). This data set is thus less affected by solar plasma and it shows daily variations of the residuals". The analysis of residuals shows the presence of significant diurnal periodic terms with the periods measured with respect to a day = 86 400 s. Their spectral analysis of the periodic terms yields the following measured periods: T1 = 0.9974 ± 0.0004 day, T2 = (1/2)(0.9972 ± 0.0004) day and T3 = 189 ± 32 days. "As T = 0.997 day = 1.0 sidereal day, these periods are consistent, (*within 0.02 percent*), with variations of one sidereal day, half a sidereal day, and half a year." (Year/2 = 182.5 days) [Our italics]. These results clearly indicate that the periodic terms in the Doppler residuals are not produced by on-board phenomena or due to solar corona affecting transmission signals, but rather that

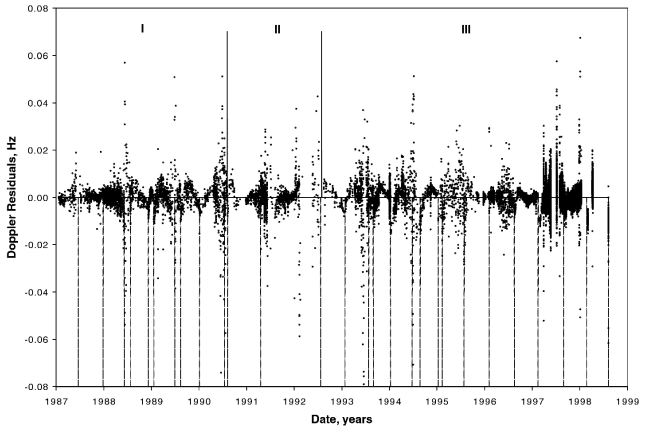

Fig. 6: "ODP Doppler residuals in Hz for the entire Pioneer 10 data span. The two solid vertical lines in the upper part of the plot indicate the boundaries between data Intervals I/II and II/III, respectively. Maneuver times are indicated by the vertical dashed lines in the lower part of the plot." [3, Fig. 13, p. 25].

they are intimately related to Earth movement relative to the Pioneer position in the sky. To illustrate their results we reproduce below (Fig. 7) a section of Figure 3 in that report.

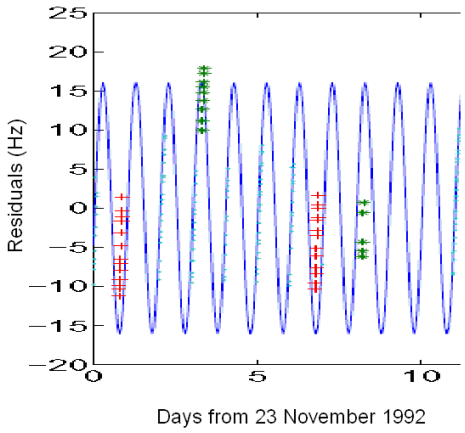

Fig. 7: Fitted residuals of the Doppler tracking data of Pioneer 10, for a 10-day period near opposition. Different symbols or colors refer to different couples of receiving stations [6, expanded section of Figure 3, p. 6]

All of the reports shown above use the original data and do not include the early stage of the Pioneer missions. It has been stated in several reports [6, 20, 24] the convenience to recover and analyze the data from the beginning of the missions. A very commendable effort has been made to recover the earlier data, which after considerable effort, has been secured in modern digital media. A detailed report of this contribution is found in [22, p. 4]. However, to our knowledge, the required detailed analysis of the earlier stages has not been

reported.

At the present times, Pioneer 10 is in the constellation of Taurus. The current Right Ascension of Pioneer 10 is 05h 16m 17s and the Declination is $+26^{\circ}02'40''$. Pioneer 11 is currently in the constellation of Scutum. The current Right Ascension of Pioneer 11 is 18h 53m 32s and the Declination is $-08^{\circ}42'43''$ [25].

3 Pioneer anomaly "constant" term

In this section, we review the theory of the calculation of the Pioneer 10 and 11 anomalous "constant" term. We start with the statement of the Céspedes-Curé Hypothesis [26, p. 279], [4, 27–29] Eq. (1): The speed of light on Earth's surface at 1 AU (S Sun, E Earth) is given by

$$c = \frac{k}{\sqrt{\rho}} = \frac{k}{\sqrt{\rho^* + \rho_S + \rho_E}} \tag{1}$$

where k is a proportionality constant and ρ the energy density in $\mathrm{J/m^3}$ on the surface of the Earth which is a sum of the contribution of the constant energy density due to far away stars and galaxies ρ^* and the constant values due to the Sun ρ_S and Earth ρ_E given by (2) below. Calculation shows that the contribution of the Moon and other planets are negligible.

The energy density of a mass [26, p. 163], [2, Eq. (2), p. 50], [4] is given by

$$\rho = \frac{GM^2}{8\pi r^4} \tag{2}$$

where G is Newton's gravitational constant, M is the mass and r is the distance from the mass center. Eq. (2) shows the energy density of a mass decreases very rapidly due to the r exponent of 4 in the denominator.

The speed of light far away from Earth and the Sun, at Pioneer's position, is given by

$$c' = \frac{k}{\sqrt{\rho'_{far}}}\,. \tag{3}$$

Here ρ'_{far} is the energy density at the site of Pioneer. In (3), ρ'_{far} contains a sum of the gravitational energy density of the far away stars and galaxies ρ^*, the Sun's and the energy density of other planets, which are relatively near in the spacecraft's trajectory towards outer space. These include the Earth in the very early stage of the mission and any planets during flyby or relative close approach, which includes the Jupiter flyby, the Saturn flyby and possibly near encounters to other planets. Hence

$$\rho'_{far} = \rho^* + \frac{G}{8\pi}\sum_{i=1}^{n}\frac{M_i^2}{r_i^4}\,. \tag{4}$$

Figs. 8 and 9 shown below give an indication of these encounters. A close look at these figures clearly shows that the gravitational energy density and gravitational acceleration along the trajectory of Pioneer 10 and 11 are different predicting different values of the anomalous acceleration as is reported.

The index of refraction of space, relative to the vacuum index on Earth, at Pioneer's position is obtained using (1) and (3):

$$n' = \frac{c}{c'} = \frac{\sqrt{\rho'_{far}}}{\sqrt{\rho}}\,, \tag{5}$$

so that the speed of light far away is:

$$c' = c\,\frac{\sqrt{\rho}}{\sqrt{\rho'_{far}}}\,. \tag{6}$$

Eq. (6) implies that c' is *greater* than c and increases with distance as ρ'_{far} decreases with distance. However, c' becomes almost constant when Pioneer goes past the planets and their energy density becomes negligible. The Sun's contribution continues to decrease leaving ρ^*, the constant energy density of far away stars and galaxies

Spacecraft velocity and accelerations are measured basically with the Doppler formula $\Delta f = f\,(v/c)$ where f would be a spacecraft-generated signal. However, Pioneer spacecraft did not have an accurate oscillator onboard. Communication uplink from Earth is at $\sim$ 2.11GHz. The spacecraft's coherently received signal is accurately multiplied by the (240/221) ratio and signals beamed at approximate downlink frequency 2.295 GHz. The signals are sent and received by the Deep Space Network (DSN) and processed in the manner described in detail by Anderson *et al* [3, pp. 7–12]. In this manner, the observable is a very precise Doppler shifted frequency $\Delta f = (f/c)(dl/dt)$ [3, p. 9, Eq. (1)], where l is the overall optical distance. In our notation $v = (dl/dt)$ so that the spacecraft speed is obtained with:

$$\vec{v} = \frac{c\Delta f}{f}\,\frac{\vec{r}}{|r|}\,. \tag{7a}$$

Differentiating (7a) with respect to time, the measured spacecraft acceleration is

$$\vec{a}_{JPL} = \frac{d\Delta f}{dt}\,\frac{c}{f}\,\frac{\vec{r}}{|r|}\,. \tag{7b}$$

Here Δf is the shift of the frequency f and $\dfrac{d\Delta f}{dt}$ the measured drift of the frequency due to the Pioneer acceleration produced by gravitation at the spacecraft site, mainly due to the Sun. $\vec{a}_{JPL}$ is a derived acceleration vector in the direction of the gravitational force causing it. Examination of (7a) and (7b) shows that, if the velocity of light c is not invariant but rather given by (6) as proposed in this work, measurement of velocity and acceleration in locations of space with lower

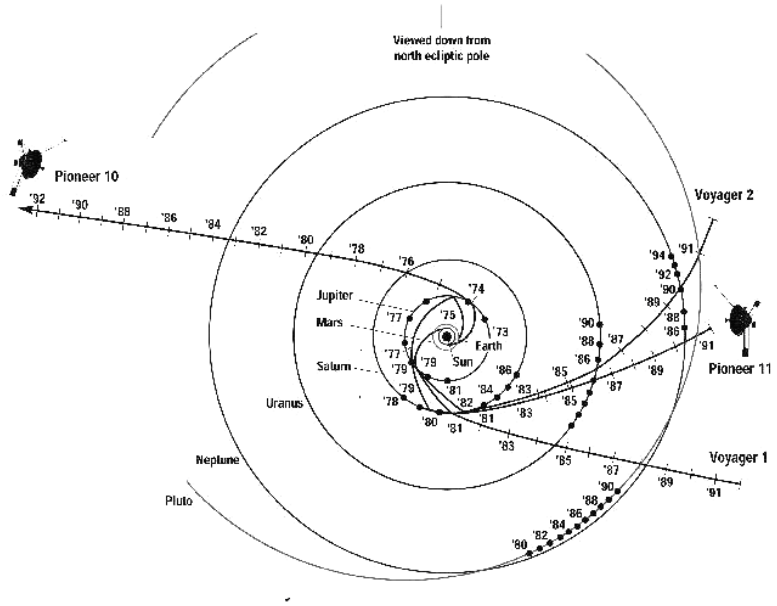

Fig. 8: "Ecliptic pole view of Pioneer 10, Pioneer 11, and Voyager trajectories. Pioneer 11 is traveling approximately in the direction of the Sun's orbital motion about the galactic center. The galactic center is approximately in the direction of the top of the figure." [3, p. 5].

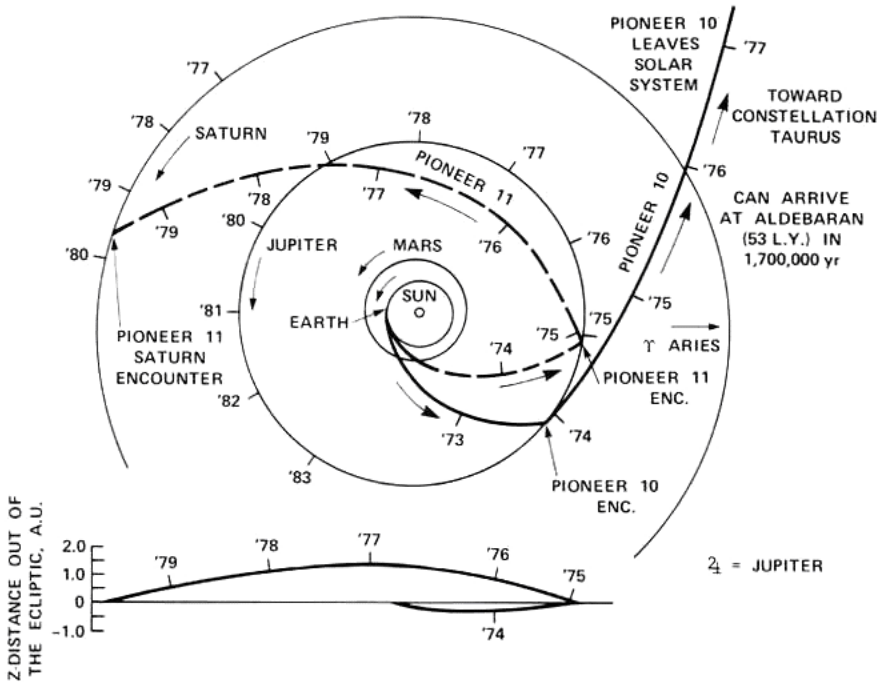

Fig. 9: Detail of early trajectories [6, p. 3].

gravitational energy density than on Earth's surface, both result in overestimation of these quantities. This leads to the belief that an anomalous acceleration towards the sun is acting.

At this point it is instructive to mention that c' differs very little from c and the magnitudes of n', the index of refraction of space, that are predicted with (5) are very nearly equal to 1. The values of n' on the surface of planets differ from Earth's

Planet	n'	Planet	n'
Mercury	0.99997382	Saturn	100.000.349
Venus	0.99999527	Uranus	0.99999524
Earth	100.000.000	Neptune	100.000.737
Mars	0.99997758	Pluto	0.99997385
Jupiter	100.014.145	Moon	0.99997454

Table 3: Values of the vacuum index of refraction n' on the surface of the planets and the Moon. The value of $\rho^* = 1.09429 \times 10^{15}\,\mathrm{J/m^3}$ calculated by Céspedes-Curé [26, p. 279] was used in evaluating n' with (5).

by very little. Table III from [4] shows the results of calculating n' with the use of (5). The values of the planets are close to 1.0 being caused by the local gravitational energy density being not too different from the surface of the Earth.

The correct value of Pioneer's acceleration is obtained with Newton's gravitational force:

$$\vec{a}_N = G \sum_{i=1}^{n} \frac{M_i}{r_i^2} \frac{\vec{r}}{|r|} . \tag{8}$$

Here the acceleration of gravity (i = Sun and planets) is mainly from the Sun, but in the early stages of the mission it will be affected by other planets which are relatively near during energy assist maneuvers (flyby) or near encounter in its trajectory towards outer space.

The Pioneer acceleration is measured with the Doppler formula (7b) with the accepted value c of the speed of light and the uplink $f = 2.113\,\mathrm{GHz}$ frequency. If instead of c we use the speed of light c' given by (6), we get a corrected Doppler-derived acceleration:

$$\vec{a}' = \frac{d\Delta f}{dt} \frac{c}{f} \frac{\sqrt{\rho}}{\sqrt{\rho'_{far}}} \frac{\vec{r}}{|r|} . \tag{9}$$

The difference between the acceleration $\vec{a}'$ as proposed here in (9) and $\vec{a}_{JPL}$ calculated with (7b) gives the predicted anomalous acceleration:

$$\vec{a}_P = \frac{d\Delta f}{dt} \frac{c}{f} \left(\frac{\sqrt{\rho}}{\sqrt{\rho'_{far}}} - 1 \right) \frac{\vec{r}}{|r|} . \tag{10}$$

4 Pioneer annual and diurnal residuals

Here, we present the theory to calculate the harmonic Doppler residuals of the Pioneer 10 and 11 spacecraft. Due to Earth's rotation and translation, the measured acceleration a_{JPL}, has superimposed Doppler shifts due to the components of these movements in the direction of the spacecraft. They are incorporated in the models used to predict the spacecraft movement by the standard galilean addition of velocities, to the predictions of gravitational theory.

We treat first the effect of Earth's rotation. Let V_{ER} be the equatorial tangential velocity (≃0.4 km/s). At the latitude λ of the DSN antennas, the tangential velocity in the direction of Pioneer changes by $\cos\lambda$. As the day progresses, the component decreases by the factor $\cos(\omega_R t + \phi_R)$, where ω_R is the Earth's *sidereal* angular rotation velocity and ϕ_R an Earth rotational phase angle. Hence the rotational Earth's velocity in the direction of Pioneer is

$$v_E = v_{ER} \cos\lambda \cos(\omega_R t + \phi_R) . \tag{11}$$

For argument's sake, we take $(\omega_R t + \phi_R)$ to be equal to 0 degrees when Pioneer is just in the East of the DSN station. Then $\cos(\omega_R t + \phi_R) = 1$ and the velocity predicted is maximum when Pioneer is in the East horizon of the DSN antenna. The component reaches a null value when Pioneer is in the zenith of the DSN station $(\omega_R t + \phi_R) = 90^{\mathrm{o}}$, and becomes negative, reaching a maximum negative value when it is exactly in the West sky of the DSN station. This component has to be added to the speed of light in (10).

In regards to Earth's translation about the Sun, let v_{ET} be Earth's translation velocity (approx. 30 km/s). The component of the translation velocity in the direction of Pioneer is

$$v_E = v_{ET} \cos\lambda \cos(\omega_T t + \phi_T) \tag{12}$$

with ω_T the Earth's sidereal angular translational velocity about the Sun and ϕ_T an Earth translational phase angle.

This component is a maximum when Pioneer is in quadrature and becomes null when it is in opposition (Sun, Earth, Pioneer alignment) or in conjunction with the Sun (Earth, Sun, Pioneer alignment). See Fig. 10.

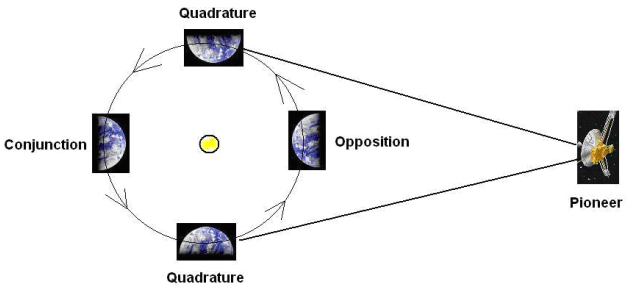

Fig. 10: The Earth translation under the position of Pioneer.

To calculate the annual and diurnal Doppler residuals, we use the galilean velocity addition as demonstrated by Gift [18] adding *to the speed of light* in (10) the Earth's orbital translation and rotational velocity

$$\vec{a}_P = \frac{d\Delta f}{dt} \frac{1}{f} \Big(c + v_{ET} \cos\lambda \cos(\omega_T t + \phi_T) + \\ + v_{ER} \cos\lambda \cos(\omega_R t + \phi_R) \Big) \left(\frac{\sqrt{\rho}}{\sqrt{\rho'_{far}}} - 1 \right) \frac{\vec{r}}{|r|} . \tag{13}$$

In order to calculate $\vec{a}'_P$ with (13) as a function of distance, it is necessary to know the frequency drift $d\Delta f/dt$. The value of the frequency drift for different distances is not available. It has been measured and considered to be constant for the later part of the trajectories. Nevertheless, its value is important for calculating the earlier part of the trajectories. We see that it is possible to calculate values by equating the correct newtonian acceleration given by (8) to the measured acceleration given by (7b). Solving for the frequency drift we obtain:

$$\frac{d\Delta f}{dt} = \frac{f}{c} G \sum_{i=1}^{n} \frac{M_i}{r_i^2} . \tag{14}$$

Here we have to use an invariant c as used by JPL.

On page 16 of Anderson *et al* (2002), it is stated that the measured frequency in Hz is converted to Doppler velocity by the use of their Eq. (13), namely $v = c\,\Delta f/2f$ in our notation. This indicates that the values reported are obtained using a *double* Doppler (uplink–downlink) velocity. Hence our formulation for the frequency shift has to be multiplied by a factor of 2:

$$\frac{d\Delta f}{dt} = \frac{2f}{c} G \sum_{i=1}^{n} \frac{M_i}{r_i^2} . \tag{15}$$

With (15) in (13) we get:

$$\begin{aligned} \vec{a}'_P = 2\Bigg[1 + \frac{v_{ET}}{c} \cos\lambda \cos(\omega_T t + \phi_T) + \\ + \frac{v_{ER}}{c} \cos\lambda \cos(\omega_R t + \phi_R)\Bigg] + \\ + G \sum_{i=1}^{n} \frac{M_i}{r_i^2} \left(\frac{\sqrt{\rho}}{\sqrt{\rho'_{far}}} - 1 \right) . \end{aligned} \tag{16}$$

Eq. (16) predicts both the constant term of the Pioneer anomalous acceleration towards the Sun and the smaller harmonic Doppler residuals in units of acceleration (m/s^2). It predicts different values for Pioneer 10 and 11 with the differences notably contained in the gravitational acceleration acting on the spacecraft (particularly during planetary encounters in the early phase of the missions). This difference is also due to the distances contained in the ρ'_{far} factor, and the different phase angles ϕ_T for the two spacecrafts.

Since they are going in different directions in the ecliptic plane, the difference $\Delta\phi = \phi_{TPio10}$ - ϕ_{TPio11} should be equal to the difference of their Right Ascensions. This is a variable quantity during the early phase of the mission. However, at the present time, it is nearly constant and equal to (Pioneer 10: 05h 16m 17s) – (Pioneer 11: 18h 53m 32s) = 204.3 degrees.

The much higher translational velocity v_{ET} of Earth with an annual period dominates over the smaller diurnal variations of $\vec{a}'_P$. However the annual variations are slow and the Earth–Pioneer component of v_{ET} is very small during conjunction and opposition.

Figure 4 from Anderson *et al* (2002) [3] clearly shows the harmonic Doppler residuals after subtracting the constant term. These figures are made up of very many different measurements without any established periodicity. Measurements were made when the probe was in the sky of one of the DSN station antennas at arbitrary times of the rotational and translational positions of Earth, which means for (16), different values of the rotational and translational phase angles ϕ_R and ϕ_T.

There are 3 DSN Stations located approximately 120 degrees apart (Madrid, Spain, Goldstone, California and Camberra, Australia). This means that measurements from each station differ in phase angle ϕ_R by about 120 degrees so that in general, it is not expected that Doppler residuals exhibit an oscillatory continuity for any length of time. Nevertheless, as mentioned and reviewed in Section 2 above, previous workers have made detailed analyses of these harmonic Doppler residuals taking into account the phase differences.

We may also derive the Pioneer annual and diurnal Doppler residuals in units of velocity or alternatively in units of frequency as has been reported [3, 9, 22].

The Doppler formula is

$$\Delta f = \frac{v_P}{c} f \tag{17}$$

with v_p the speed of the Pioneer spacecraft, f the transmitting frequency, Δf the frequency change and c the speed of light considered a constant. In the case of the Pioneer spacecraft, it is a "Double" Doppler effect as mentioned above, hence:

$$\Delta f = 2\,\frac{v_P}{c} f . \tag{18}$$

If, instead of c, we use c plus the Earth speed following the results of Gift (2017) [18], then we write

$$\Delta f'' = 2\,\frac{v_P}{c + v_E} f . \tag{19}$$

NASA expects (18) and gets Δf plus or minus a "residual" which we think is due to not using (19). Hence the residual must be (18) minus (19):

$$\Delta f'' = \Delta f - \Delta f' = 2 v_P f \left(\frac{1}{c} - \frac{1}{c + v_E} \right) . \tag{20}$$

Or

$$\Delta f'' = 2 v_P f \left(\frac{v_E}{(c^2 + c v_E)} \right) .$$

This approximates to

$$\Delta f'' \approx 2 v_P f \left(\frac{v_E}{c^2} \right) . \tag{21}$$

This relation gives the maximum values. To calculate the diurnal Doppler residuals as a function of time, we substitute (11) in (21):

$$\Delta f''_D \approx 2f\,\frac{v_P\, v_{ER}}{c^2} \cos\lambda \cos(\omega_R t + \phi_R) . \tag{22a}$$

The equivalent relation for annual residuals is obtained by substituting (12) in (21)

$$\Delta f_A'' \approx 2f \frac{v_P v_{ET}}{c^2} \cos\lambda \cos(\omega_T t + \phi_T) . \qquad (22b)$$

The result (22) gives the annual and diurnal residuals $\Delta f''$ in units of frequency (Hz). We want to compare with results in velocity units such as (mm/s) as shown in Fig. 4. To convert from Hz to m/s Anderson *et al* (2002) [3, p. 16] uses

$$\Delta v'' = \frac{\Delta f'' c}{2f} . \qquad (23)$$

Then substituting (22) in (23) we get for the diurnal Doppler residuals in [m/s]:

$$\Delta v_D'' = \frac{v_P\, v_{ER}}{c} \cos\lambda \cos(\omega_R t + \phi_R) . \qquad (24a)$$

The equivalent relation for annual residuals is

$$\Delta v_D'' = \frac{v_P\, v_{ET}}{c} \cos\lambda \cos(\omega_T t + \phi_T) . \qquad (24b)$$

5 Results

In this section we use the theory developed above to predict qualitatively and quantitatively the reported Pioneer Anomaly "constant" and harmonic Doppler residuals.

5.1 Pioneer 10 anomaly at 20 AU

At 20 AU we calculate the anomalous acceleration with (16). For this "constant" term, we omit the terms dealing with the harmonic Doppler residuals and consider only the gravitational acceleration and energy density (in ρ'_{far}) due to the Sun and Earth:

$$\vec{a}_P = 2G\left(\frac{M_S}{r_S^2} + \frac{M_E}{r_E^2}\right)\left(\frac{\sqrt{\rho}}{\sqrt{\rho'_{far}}} - 1\right)\frac{\vec{r}}{|r|} . \qquad (25)$$

This expression predicts:

$$a_P = 7.754 \times 10^{-8}\,\mathrm{cm/s^2} . \qquad (26)$$

This calculated value differs by just 1.2 percent from the value $a_P = 7.85 \pm 0.02 \times 10^{-8}\,\mathrm{cm/s^2}$ reported by O. Olsen (2007) [7] in an independent analysis of the Pioneer 10 data for Interval I. The value calculated in (26) also coincides, within the error estimation, with the result quoted by Anderson *et al* (2002) [3, p. 24]: "1-day batch-sequential estimation for the entire data interval of 11.5 years for Pioneer 10 (*which*) yielded a result $a_P = (7.77 \pm 0.16) \times 10^{-8}\,\mathrm{cm/s^2}$." In this case our calculation differs by just −0.2 percent.

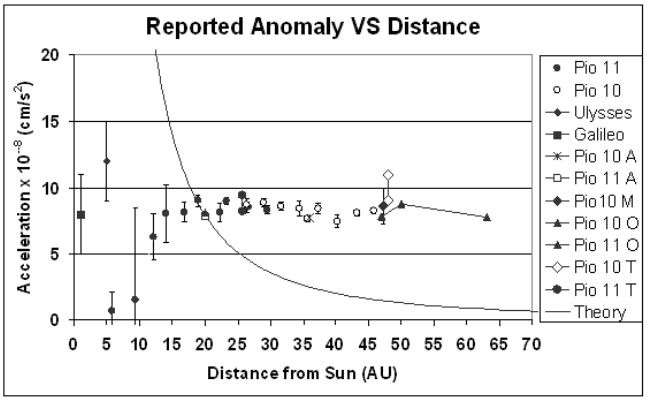

Fig. 11: Anomalous acceleration $\times\ 10^{-8}$ in units of (cm/s^2) as a function of distance from the Sun. Values of anomalous acceleration reported and reviewed above are plotted with the theoretical line according to (25) (A Anderson, M Markwardt, O Olsen, T Toth).

5.2 Pioneer anomaly as a function of distance from the Sun

To present the anomalous acceleration predicted as a function of distance, we show below results of a simple model with the influence of the Sun and Earth ignoring the other planets.

The theoretical curve in Fig. 11 shows a variable slope decreasing with distance. V. Toth (2009) reports in his independent analysis, as quoted above, values for a_P variation rates for Pioneer 10 and 11. However, it is not stated for what distances or dates are these quantities deduced. The value reported for Pioneer 10 [22, p 20] is $da_{P10}/dt = -(0.21 \pm 0.04) \times 10^{-6}\,\mathrm{cm/s^2/year}$. We find that the theoretical curve in Fig. 11 exhibits that slope exactly, within the uncertainty shown, at a distance between 42 and 48 AU.

For Pioneer 11, the Toth reported variation rate is $da_{P11}/dt = -(0.34 \pm 0.12) \times 10^{-8}\,\mathrm{cm/s^2/year}$. We find that the theoretical curve in Fig. 11 exhibits that slope exactly, within the uncertainty shown, at distances between 29 and 38 AU. Hence, we fully agree with Toth's comment: "an anomalous acceleration that is a slowly changing function of time (*decreasing*) cannot be excluded at present" [our italics].

5.3 Pioneer anomaly during Jupiter flyby

Ulysses, Pioneer 10 and 11 had close encounters with Jupiter as part of mission exploration objectives and for orbit modifications or energy assistance maneuvers. We show now how the theory developed here can explain some of the observations reported during Jupiter flyby by these spacecrafts. The effects of the gravitational energy density due to the planets are very short range according to (2) and even for the Sun [4]. Likewise the gravitational acceleration produced by the planets is relatively short range compared to the large distances traversed by these spacecrafts. To put the values in perspective, we show in Fig. 12 the gravitational acceleration of the

Sun and the planets each centered about their orbital distance to the Sun.

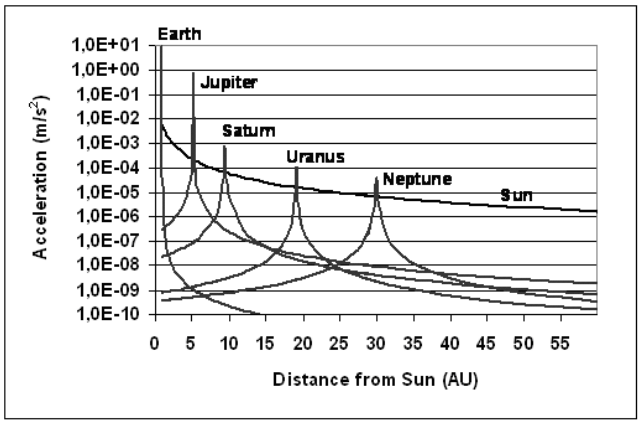

Fig. 12: Gravitational acceleration of the Sun, Earth and planets centered about the position of their orbits about the Sun. (Values are calculated to within 0.2 AU of each planet, and centered at nominal orbital distance).

Fig. 12, top line, shows that compared to the gravitational acceleration of the Sun the planet's acceleration affects only their immediate vicinity. If we rewrite (16) considering just the Sun and Jupiter and emphasizing the vectorial character of $\vec{a}_P$, we get

$$\vec{a}_P = 2G\left(\frac{\sqrt{\rho}}{\sqrt{\rho'_{far}}} - 1\right)\left(\frac{M_S}{r_S^2}\,\frac{\vec{r}}{|r_S|} + \frac{M_J}{r_J^2}\,\frac{\vec{r}}{|r_J|}\right). \qquad (27)$$

Figs. 13 and 14 show the Jupiter flybys of the Pioneer spacecraft. Judging from the incoming and outgoing trajectories towards Jupiter in the polar view of the Pioneer 11 flyby, we deduce that the resulting vectorial gravitational acceleration due to Jupiter and the Sun was mainly in the direction of the Sun, but with the gravitational attraction of Jupiter in the opposite direction. Hence the initial two points in the Pioneer 11 anomalous acceleration (see Fig. 2) which, as reported by Nieto and Anderson (2005) [6], correspond to a time when the spacecraft was under the gravitational attraction of Jupiter and Saturn, are expected to be of a smaller magnitude and additionally, exhibit a large error due to the measurement of a fast changing quantity as they cross the gravitational field of the planets.

In regards to the Pioneer 11 Saturn flyby, we can rewrite (27) in terms of the planet's gravitational field:

$$\vec{a}_P = 2G\left(\frac{\sqrt{\rho}}{\sqrt{\rho'_{far}}} - 1\right)\left(\frac{M_S}{r_S^2}\,\frac{\vec{r}}{|r_S|} + \frac{M_{Sat}}{r_{Sat}^2}\,\frac{\vec{r}}{|r_{Sat}|}\right). \qquad (28)$$

Toth and Turyshev (2007) [20, p. 15] comment about the Pioneer 11's Saturn encounter:

> ...for Pioneer 11, a small value for the anomaly was found during the Jupiter–Saturn cruise phase. Right at the time of the Saturn encounter, however, when the spacecraft passed into a hyperbolic escape orbit, there was a rapid increase in the anomaly, whereafter it settled into the canonical value.

Unfortunately, no numerical values are quoted. However, in the light of Fig. 15 and (28) this text can be explained: When the spacecraft was in the incoming Saturn flyby, it went from an area of gravitational acceleration towards the Sun to an area of stronger gravitational acceleration towards Saturn. This has the effect of decreasing a_P until closest encounter.

Furthermore, as the spacecraft nears the planet it goes from the interstellar gravitational energy density (relatively low) and enters the area of Saturn's energy density with the highest value just at nearest encounter. In this area, $n' = \sqrt{\rho}\,/\,\sqrt{\rho'_{far}}$ increases towards a value similar to Earth's (see the value of n' for Saturn in Table I). Hence, the first term in brackets in (28) decreases rapidly until the nearest point to Jupiter and then increases rapidly settling in the interstellar n' value. This is precisely as reported by Toth and Turyshev.

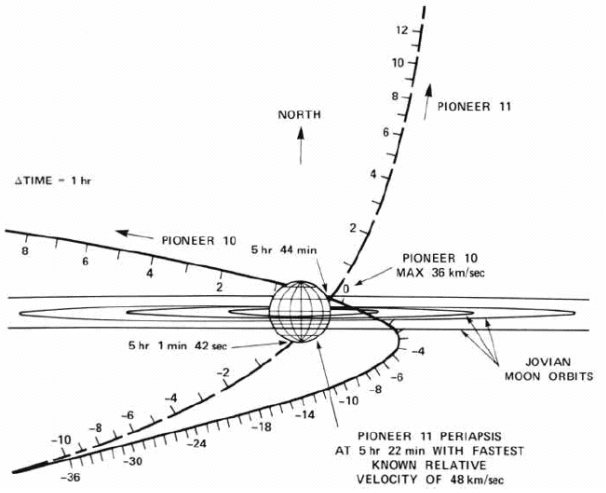

Fig. 13: The Jupiter Flyby of the Pioneer spacecraft, equatorial view [6, Fig. 2, p. 3].

5.4 Pioneer diurnal and annual Doppler residuals

In (16), the diurnal and annual residuals are essentially contained in the first bracket, namely

$$\left(1 + \frac{v_{ER}}{c}\,\cos\lambda\cos(\omega_R\,t + \phi_R) + \frac{v_{ET}}{c}\,\cos\lambda\cos(\omega_T\,t + \phi_T)\right)$$

which multiplies the "constant" term.

The term $\cos\lambda$ is the cosine of the DSN latitude. The latitude of the three stations are Goldstone = 35.4267° N, Madrid

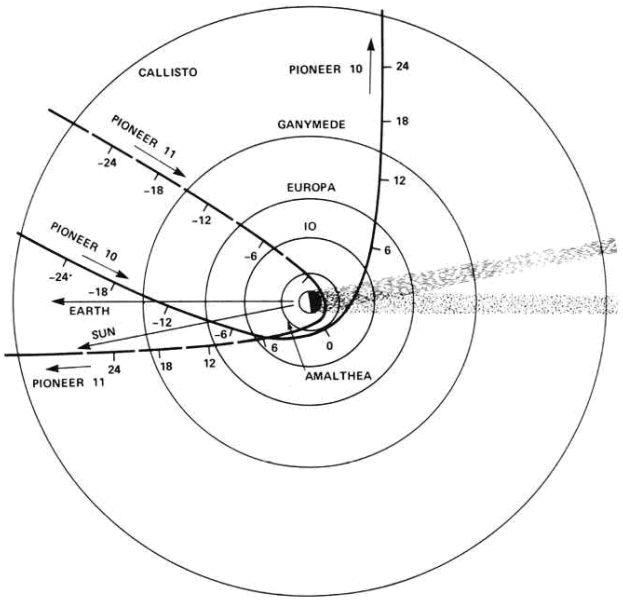

Fig. 14: The Jupiter Flyby of the Pioneer spacecraft. Polar view. From [6, Fig. 2, p. 3].

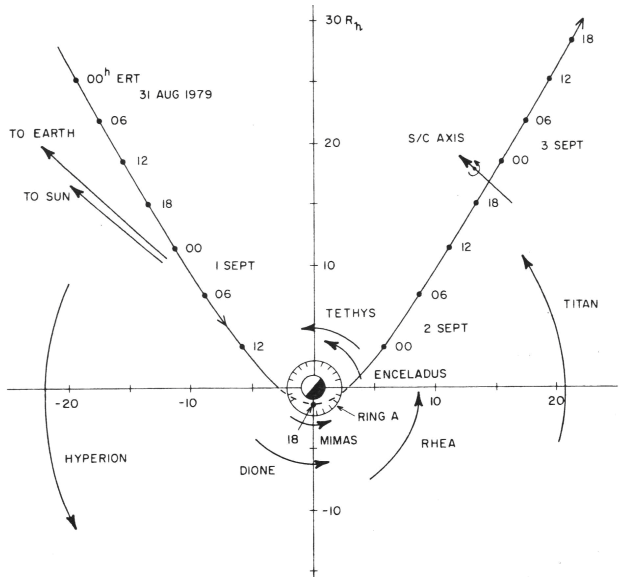

Fig. 15: Pioneer 11 Saturn flyby on the 1st of September 1979. From [6, Fig.3, p. 6].

= 40.4314° N, and Canberra = 35.4013° S. We take the average 37.0864 so that the term $\cos\lambda = 0.79772$. If we substitute the Earth's equatorial rotational velocity $v_{ER} = 465.1$ m/s [30] and Earth's translational velocity $v_{ET} = 2.978 \times 10^4$ m/s and multiply by $\cos\lambda$, we get the following expression:

$$\Big(1 + 1.22402 \times 10^{-6} \cos(\omega_R t + \phi_R) + \\ + 7.92424386 \times 10^{-5} \cos(\omega_T t + \phi_T)\Big). \quad (29)$$

The "cos" term on the left describes the diurnal Doppler residuals with $\omega_R = 7.292 \times 10^{-5}$ rad/s, the Earth's sidereal angular rotation, and the "cos" term on the right describes the annual Doppler residuals with $\omega_T = 2.020$ x 10^{-7} rad/s, the Earth's sidereal angular rotation around the Sun. The sum of the three terms in (29) is very nearly equal to unity. For example, for the maximum amplitude of both oscillatory terms we get (29) to be: 1.00008046. On the other hand at opposition (Sun, Earth and Pioneer in that order) the third translational term is null and the maximum oscillatory term is due to Earth rotation and equal to 1.000001224.

The actual amplitude of the oscillations is obtained by multiplying (29) by the "constant" term in (16). As we have shown above, this is a variable value that depends on the distance to the Sun and also to the planets during encounters or flyby maneuvers. Hence to compare accurately with reported values, it is required to know at what distance or on what date were the measurements made.

5.4.1 Annual residuals

To compare with the Pioneer 10 sine wave reported, Fig. 4, we consider that for Pioneer 10 the data spans a distance from approximately 25 to 45 AU (as reported in Fig. 3). The result of multiplying the maximum amplitude of the oscillatory terms due to Earth's translation velocity, 1.00007924, by the calculated anomaly in this distance range, results in 5.1 to 1.6×10^{-8} cm/s^2. These values compare favorably to the amplitude of the annual oscillatory term reported by Anderson *et al* (2002) [3, p. 40] of "about 1.6×10^{-8} cm/s^2". However, they are larger than the estimate given by the same authors on [3, p. 14]: "the best estimate of the amplitude of the Pioneer 10 sine wave is $(0.525 \pm 0.155) \times 10^{-8}$ cm/s^2 and that of the Pioneer 11 wave is $(0.498 \pm 0.176) \times 10^{-8}$ cm/s^2. These values have a systematic error of $\sigma_{at} = 0.32 \times 10^{-8}$ cm/s^2" as reported for the entire Pioneer data span by Turyshev and Toth (2009) [24, p. 86].

The reported angular velocity of the annual Doppler residuals is approximately 2×10^{-7} rad/s. This value coincides with the Earth's sidereal translational rotation velocity which is 2.0200×10^{-7} rad/s as proposed in this work.

Figs. 5 and 6 show clearly the measured annual residuals. We wish to compare the results of the theory above to the undulating information contained in Fig. 5. To that end, we write the last term in (29) that deals with the annual Doppler residuals as a function of time for Pioneer 10 as:

$$(1 + 7.92424 \times 10^{-5} \cos(2.020 \times 10^{-7} t + \phi_R)) \quad (30)$$

where $\omega_T = 2.020 \times 10^{-7}$ rad/s is the Earth's angular rotation around the Sun.

Eq. (30) has to be multiplied by the calculated anomalous acceleration a_P. This value changes with distance as shown in Fig. 11. From 42 to 63 AU, the predicted anomaly calcu-

lated with (25) ranges from (1.84 to 0.837) $\times 10^{-8}$ cm/s^2 respectively. Hence we chose to select the middle of the three distance intervals as shown in Table IV (distance values derived using data in Fig. 3).

Interval	Dates	Mid date	Mid distance (AU)	Predicted a_P (10^{-8} cm/s^2)
I	1887-1990	1988.5	43	1.758
II	1990-1992	91	52	1.214
III	1993-1998	95.5	63	0.837

Table 4: Predicted a_P for the mid-distance of Pioneer 10 intervals. Values that were chosen to calculate the annual residuals.

Fig. 16 shows the agreement between the calculated annual Doppler residuals and the published results. The amplitude of the predicted oscillations are larger in interval I and decrease in intervals II and III as is reported by Anderson *et al* (2002): "At early times the annual term is largest. During Interval II, the interval of the large spinrate change anomaly, coherent oscillation is lost. During Interval III the oscillation is smaller and begins to die out." [3, p 40].

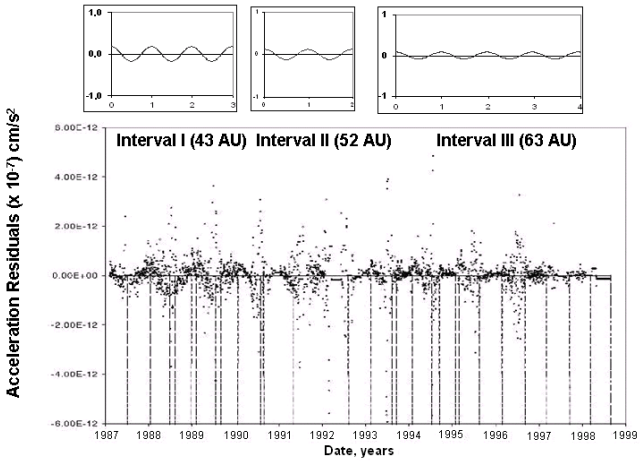

Fig. 16: Comparison of reported annual residual undulations with the predicted Doppler residuals. For uniformity, the original scale in units of [km/s^2] [3, Fig. 17, p. 40], is shown in units of [cm/s^2 $\times$ 10^{-7}]. Inlays plots were drawn to approximately the same X–Y scale as the original data and show the predicted decreased calculated amplitudes corresponding to the center of each of the three intervals.

5.4.2 Diurnal residuals

Levi *et al* (2009), in their spectral analysis of the periodic terms yields the following measured periods: T1 = 0.9974 ± 0.0004 day, T2 = (1/2)(0.9972 ± 0.0004) day and T3 = 189 ± 32 days. As T = 0.9972 day = 1.0 sidereal day, these periods are consistent, within 0.02 percent, with variations of one sidereal day, half a sidereal day, and half a year.

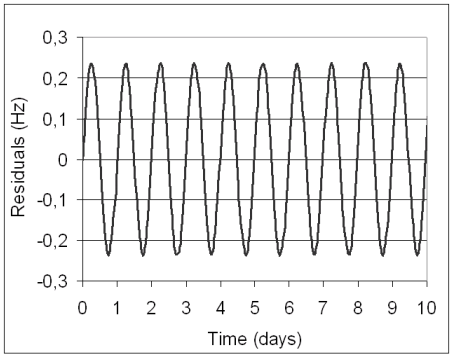

Fig. 17: Diurnal Doppler residuals calculated with (22).

The diurnal oscillations reported by Levi *et al* (2009) [9] between 23 November 1996 to 23 December 1996, reviewed above in Fig. 7 were at an estimated distance of 66.73 to 66.96 AU from the Sun (determined by the use of Fig. 3). Also, they were done at opposition, so that the annual rotational term is almost null and solar coronal influence is minimized.

The diurnal Doppler residuals in frequency units (Hz) may be calculated with (22a) namely:

$$\Delta f_D'' \approx 2f \frac{v_P\, v_{ER}}{c^2} \cos\lambda \cos\left(\omega_R t + \phi_R\right).$$

In this relation the speed of Pioneer v_P at a distance of 66.8 AU was estimated at 12 500 m/s and with the Earth's equatorial rotation velocity of 465.1 m/s, (22) leads to the oscillations shown in Fig. 17 next to the oscillations reported by Levi *et al* [9] in Fig. 18.

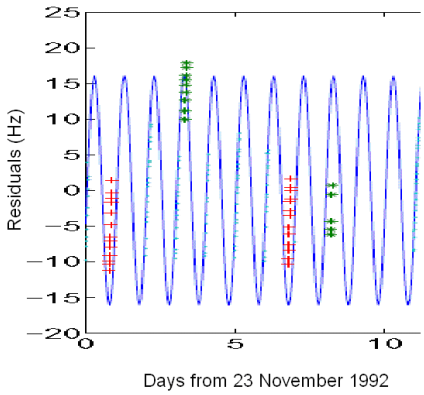

Fig. 18: Diurnal Doppler residuals reported by Levi *et al* [9].

We see that the frequency of diurnal oscillations reported by Levi *et al* (2009) [9] coincides with our predicted frequency $\omega_R = 2\pi f_E$, of Earth rotation, to within 0.02 percent.

A further conclusion of Levi *et al* (2009) [9, p. 10] is: "The main new result of the paper is that a large part of these diurnal and seasonal anomalies may be explained by a simple

geometrical model where the light line on the tracking path is modified in a manner depending on the azimuthal angle ϕ between the Sun-Earth and Sun-probe lines."

We reflect about this conclusion that the azimuthal angle ϕ between the Sun-Earth and Sun-probe lines will show diurnal variations superimposed on annual variations which are wholly compatible with the first bracket of (16) and expression (29) above. With the use of (24a), namely:

$$\Delta v_D'' = \frac{v_P v_{ER}}{c} \cos\lambda \cos(\omega_R t + \phi_R),$$

we can calculate the diurnal Doppler residuals in velocity units as reported by Anderson *et al* (2002) [3] and shown in Fig. 4, using the rotational velocity of Earth 465,1 m/s, and the estimated speed of Pioneer 10 in 1995 of 12 500 m/s. A comparison of the results is shown in Fig. 19 and Fig. 20.

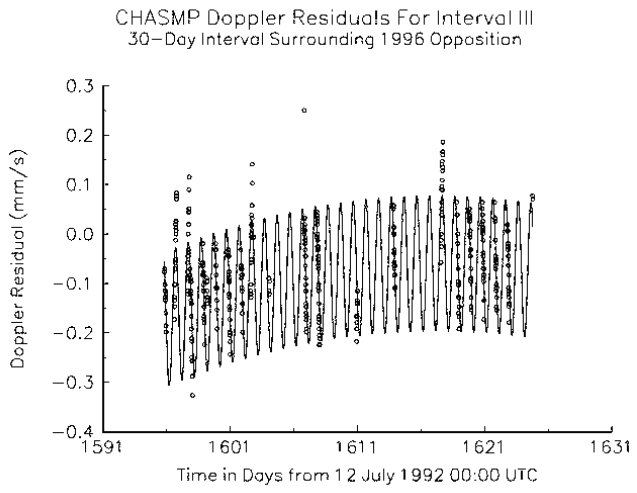

Fig. 19: Diurnal Doppler residuals in velocity units from [3, Fig. 18, p. 41].

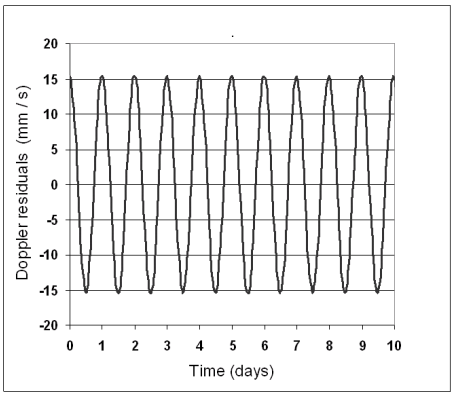

Fig. 20: Diurnal Doppler residuals in velocity units calculated with the use of (24a).

5.5 On the energy density due to far away stars and galaxies

In this work, we have used the value of $\rho^* = 1.094291 \times 10^{15}$ J/m^3, the energy density of space due to far away stars and galaxies, a value calculated by J. Céspedes-Curé [26, p 279], obtained using starlight deflection measurements during total sun eclipses. With this value in the equations, in this work, it has been possible to calculate numerically the anomalous Pioneer acceleration.

It is possible to work in the inverse order and use the empirically determined values of the anomaly to calculate in an independent way the value of this physical magnitude. When this is done, using the accurately reported Pioneer Anomaly at 20 AU, the result gives for the energy density of space due to far away stars and galaxies the value $\rho^* = 1.0838 \times 10^{15}$ J/m^3. This value differs by less than 1 percent from the value determined by J. Céspedes-Curé on the basis of a completely different phenomenon, the bending of light rays during solar eclipses.

We would like to briefly review the procedure that was published to make this determination. For details please consult [4]. The calculation uses the following formulas: Eq. (19) in [4]:

$$n' = 1 - \frac{E_D\, c}{2 f_e\, G \left(\frac{M_S}{r_S^2} + \frac{M_E}{r_E^2} \right)}, \tag{31}$$

and Eq. (8) in [4]:

$$\rho^* = \frac{\rho_{\mathrm{Sfar}} + \rho_{\mathrm{Efar}} - n'^2(\rho_{S\,1AU} + \rho_E)}{n'^2 - 1} \tag{32}$$

where (numerical values in SI units)

- n' = index of refraction of space at 20 AU (comes out to 0.999973567943846).
- ρ^* = energy density of space due to far away stars and galaxies.
- E_D = a steady frequency drift of 5.99×10^{-9} Hz/s from the Pioneer 10 spacecraft [3, p. 20].
- f_e = 2 295 MHz, the frequency used in the transmission to the pioneer spacecraft [3, p. 15].
- c = 299792458.0 m/s. Speed of light on Earth at the surface.
- $G = 6.67300 \times 10^{-11}$ m^3 kg^{-1} s^{-2}, Newton's universal constant of gravitation.
- $M_S = 1.98892 \times 10^{30}$ kg, mass of the Sun.
- $M_E = 5.976 \times 10^{24}$ kg, mass of the Earth.
- The distances r_S and r_E are the distances from the spacecraft at 20 AU (20 AU from the Sun, 19 AU from the Earth) to the center of the Sun and Earth respectively. To calculate them use was made of:

- 1 Astronomical Unit (AU) = 149 598 000 000 meters.

To calculate Eq. (8) in [4], use is made of the energy density given by our Eq. (2), namely

$$\rho = \frac{GM^2}{8\pi r^4}$$

where r is the distance from the centre of the Sun or Earth to the point where the energy density is being calculated as follows:

- for the Earth surface: $r_E = 6\,378\,140$ m, radius of the Earth.
- for the Sun at 1 AU: $r_S = 149\,598\,000\,000$ meters.
- for the Sun at 20 AU: twenty times the previous value used to calculate $\rho_{S\,far}$.
- for the Earth at 20 AU: radius of the Earth + 19 times 149 598 000 000 meters used to calculate $\rho_{E far}$.

Values were calculated with Microsoft Office Excel 2003 which uses 15 significant digits.

6 Discussion

The theoretically calculated Pioneer Anomalous acceleration shown in Fig. 11 has a decreasing value as a function of distance contrary to the generally accepted opinion that it is a "constant" value. However, the numerical evidence supplied by V. Toth (2009) [22] in his independent analysis, gives confirmation that the anomaly is a decreasing function which coincides exactly with the theoretical slope for Pioneer 11 at a distance between 29 and 38 AU and also with the theoretical slope for Pioneer 10 at a distance from the Sun between 42 and 48 AU.

At a distance from the Sun of 20 AU, the theoretical curve predicts $a_P = 7.754{\times}10^{-8}$ cm/s^2 which differs by just 1.2 percent from the value $a_P = 7.85 \pm 0.02 \times 10^{-8}$ cm/s^2 reported by O. Olsen (2007) [7] in his independent analysis of the Pioneer 10 data for Interval I. Furthermore, the theoretical value differs by just −0.2 percent from the 1-day batch-sequential estimation for the entire data interval of 11.5 years for Pioneer 10 reported by Anderson *et al* (2002) [3, p. 24] .

The theory predicts that the anomalous acceleration has a vectorial character $\vec{a}_P$ in the direction of the resultant gravitational acceleration field at the position of the spacecraft. This fact allows satisfactory explanation of the reported anomalous behavior of Ulysses, Pioneer 10 and 11 during Jupiter flyby. The observations of the peculiar values reported for the first 3 values of Pioneer 11 (see Fig. 11) are adequately explained with consideration that they correspond to the spacecraft being affected by the Jupiter gravitational acceleration which at close distances exceeds the Sun's gravitational acceleration (see Fig. 12). The prediction that the anomalous acceleration is in the direction of the resultant gravitational acceleration field at the position of the spacecraft gives an answer to this question, which is posed by several publications on the Pioneer Anomaly.

With regard to the harmonic behavior of the Doppler residuals, relaxing the assumption that the value of the speed of light c in the Doppler formula is invariant and adopting the galilean addition of the Earth rotational and translational velocity to the speed of light, results in an almost exact agreement with the measured *frequencies* for the annual (within 1 percent) and diurnal (within 0.02 percent) residuals as shown in Sections 5.4.1 and 5.4.2 above. However, the values for the magnitudes of the oscillations do not all agree as well.

In the case of the annual residuals, we do a visual comparison in Fig. 16 which agrees quite well. Particularly if we take into account that the reported values have significant errors: A systematic error of $\sigma_{at} = 0.32 \times 10^{-8}$ cm/s^2 ($\sigma_{at} = 3.2 \times 10^{-7}$ cm/s^2 in the scale of Fig. 16) is reported for the entire Pioneer data span by Turyshev and Toth (2009) [24, p. 86]. Considering the scatter of the measured values, the predicted magnitude adequately fits the data in this case.

In the case of the diurnal residuals, expressed in frequency units (Hz) as shown in Fig. 13, there is a discrepancy in the *amplitude* of the order of a factor of about 70 smaller in the calculated value of the oscillations in comparison with the amplitude of the oscillations reported by Levi *et al* [9]. With the calculated oscillations in velocity units (mm/s) the reverse is obtained. As shown in Fig. 19 the calculated amplitude is a factor of about 50 larger than the values in Fig. 4 by Anderson *et al* [3]. In view of these differences it is instructive to compare the amplitudes of the different reported values which also show significant differences.

The amplitude of the diurnal residuals in *frequency* units (Hz) reported by Levi *et al* [9, p. 6], shown in Fig. 7 are a factor of about 250 times greater than the amplitude of diurnal residuals in frequency units (Hz) reported by Anderson *et al* (2002), our Fig. 4 [3, Fig. 18, p. 41]. Both reports are for the same interval of time (23 November to 23 December 1996).

Regarding the annual residuals there is also a discrepancy in the amplitudes expressed in *acceleration* units (cm/s^2) reported by Anderson *et al* in the 2002 paper. The amplitude of the annual oscillations shown in Fig. 4 are about 10 times greater than those reported in the same paper in Fig. 12 [3, p. 26]. In view of the good agreement in the prediction of the frequencies of the harmonic Doppler residuals, it is not clear what are the sources of the discrepancies between reported amplitudes, or the differences between reported and the calculated amplitudes.

7 Conclusions

As summarized in the Discussion above, the theory presented in this work is capable of explaining qualitatively and quantitatively the phenomena associated with the Pioneer Anomaly, both, the secular and the harmonic terms that up to now had no plausible explanation. These precise calculations of the

Pioneer Anomaly, without any adjustable parameters, provide additional confirmation of the Céspedes-Curé hypothesis, that c the speed of light depends on the gravitational energy density of space as defined by (1) namely: $c = k / \sqrt{\rho}$. The highly accurate calculation of the observed frequencies of the annual and diurnal Doppler residuals and some of the amplitudes of the annual oscillations supply additional evidence that the speed of Earth adds to c, the speed of light, according to the galilean addition of velocity, thereby confirming this conclusion put forth by the analysis of S. Gift using the Global Positioning System [16–18].

The extremely accurate measurements provided by NASA as empirical data and the theoretical explanation, agreeing within 1 percent, presented in this work for the Céspedes-Curé hypothesis, have profound consequences in the current cosmology theories. The dependence of the speed of light on the gravitational energy density of space implies a revision of all astronomical measurements of velocity based on the Doppler, blue and red shifts, of stars and galaxies. These have importance in the determination of matters such as the Hubble constant, the expansion of the universe, the flat rotation curve of galaxies (which gave birth to the theory of dark matter) and the extreme values of the redshifts of very far away galaxies (so called inflation) which gave birth to the theory of dark energy.

Acknowledgements

We would like to acknowledge the independent verification of numerical calculations provided by Simon E. Greaves.

Received on June 3, 2021

References

1. Anderson J. D., Campbell J. K., Ekelund J. E., Jordan E. and Jordan J. F. Anomalous Orbital-Energy Changes Observed during Spacecraft Flybys of Earth. *Phys. Rev. Letters*, 2008, v. 100 (091102), 1–4.
2. Greaves E. D., Bracho C. and Mikoss I. A Solution to the Flyby Anomaly Riddle. *Progress in Physics*, 2020, v. 16 (1), 49–57.
3. Anderson J. D., Laing Ph. A., Lau E. L., Liu A. S., Nieto M. M. and Turyshev S. G. Study of the anomalous acceleration of Pioneer 10 and 11. *Phys. Rev. D*, 2002, v. 65 (082004).
4. Greaves E. D. NASAs astonishing evidence that c is not constant: The pioneer anomaly. arXiv: physics.gen-ph/0701130v1.
5. Turyshev S. G. and Toth V. T. The Pioneer Anomaly. arXiv: gr-qc/1001.3686v2.
6. Nieto M. M. and Anderson J. D. Using early data to illuminate the Pioneer anomaly. *Classical and Quantum Gravity*, 2005, v. 22, 5343–5354. arXiv: gr-qc/0507052v2.
7. Olsen O. The constancy of the Pioneer anomalous acceleration. *Astronomy and Astrophysics*, 2007, v. 463, 393–397.
8. Ghosh A. On the Annual and Diurnal Variations of the Anomalous Acceleration of Pioneer 10. *Apeiron*, 2007, v. 14 (3).
9. Levy A., Christophe B., Berio P., Metris G., Courty J. M. and Reynaud S. Pioneer Doppler data analysis: study of periodic anomalies. *Adv. Space Res.*, 2009, v. 43, 1538–1544. arXiv gr-qc/0809.2682.
10. Turyshev S. G., Toth V. T., Kinsella G., Lee S.-C., Lok S. M., Ellis, J. Support for the Thermal Origin of the Pioneer Anomaly. *Physical Review Letters*, 2012, v. 108 (24), 241101. arXiv: /1204.2507.
11. Bilbao L. Does the velocity of light depend on the source movement? *Prog. in Phys.*, 2016, v, 12 (4), 307–312.
12. Rievers B. and Lämmerzahl C. High precision thermal modeling of complex systems with application to the Flyby and Pioneer Anomaly. *Annalen der Physik*, 2011, v, 523 (6), 439–449.
13. Francisco F., Bertolami O., Gil P. J. S. and Páramos J. Modelling the reflective thermal contribution to the acceleration of the Pioneer spacecraft. arXiv: physics.space-ph/1103.5222v2.
14. Bilbao L., Bernal L. and Minotti F. Vibrating Rays Theory. arxiv: abs/1407.5001.
15. Greaves E. D. A Neo-Newtonian Explanation of the Pioneer Anomaly. *Revista Mexicana de Astronomia y Astrofisica*, 2009, v. 35, 23–24. ISSN 0185-1101, www.redalyc.org/articulo.oa?id=57115758008, accessed August 2021.
16. Gift S. J. G. Doppler Shift Reveals Light Speed Variation. *Apeiron*, 2010, v. 17 (1), 13–21.
17. Gift S. J. G. Time Transfer and the Sagnac Correction in the GPS. *Applied Physics Research*, 2014, v. 6 (6), 1–9.
18. Gift S, J. G. One-way Speed of Light Using the Global Positioning System. In: Torres, G., ed. Global Positioning Systems (GPS): Performance, Challenges and Emerging Technologies, Nova Publishers, NY, 2017, pp. 45–66.
19. NASA Solar System Exploration – Galileo. solarsystem.nasa.gov/missions/galileo/in-depth/, retrieved August 2020.
20. Toth V. T. and Turyshev S. G. The Pioneer Anomaly: Seeking an explanation in newly recovered data. *Can. J. Phys.*, 2007, v. 84, 1063–1087.
21. Markwardt C. Independent Confirmation of the Pioneer 10 Anomalous Acceleration. arXiv: gr-qc/0208046v1.
22. Toth V. T. Independent Analysis of the Orbits of Pioneer 10 and 11. *Int. J. Mod. Phys.*, 2009, v. D18, 717–741. arXiv: /0901.3466.
23. Levy A., Christophe B., Bério P., Métris G., Courty J.-M. and Reynaud S. Pioneer 10 Doppler data analysis: disentangling periodic and secular anomalies. *Advances in Space Research*, 2009, v. 43, 1538–1544. arXiv: gr-qc/0809.2682v2,
24. Turyshev S. G. and Toth V. T. The Pioneer Anomaly in the Light of New Data. arXiv: gr-qc/0906.0399v1.
25. Pioneer 10 coordinates: theskylive.com/pioneer10-info. Pioneer 11 coordinates: theskylive.com/pioneer11-info. Topocentric coordinates computed for the selected location of Greenwich, United Kingdom, accessed July 2021.
26. Céspedes-Curé J. Einstein on Trial or Metaphysical Principles of Natural Philosophy. et al. Organization, Caracas, Venezuela, 2002. www.nuclear.fis.usb.ve/Cespedes-Cure-2002-Einstein-on-Trial-J.pdf, retrieved 10 January 2019.
27. Greaves E. D. (2015) La hipótesis de Céspedes-Curé y el índice de refracción del espacio en un campo magnético. (The Céspedes-Curé hypothesis and the index of refraction in a magnetic field). *Acta Científica Venezolana*, 2015, v. 66 (4), 226–229.
28. Greaves E. D. The index of refraction of quasi-empty space. Unpublished, Universidad Simón Bolívar, Caracas, Venezuela, 2015. www.nuclear.fis.usb.ve/fn/wp-content/uploads/2015/07/GREAVES-ED-Index-of-refraction-of-quasi-empty-space-V11.pdf, retrieved 19 April 2019.
29. Greaves E. D. Propiedades del espacio vacío. (Properties of empty space). Memorias del II Congreso de ABAE, September 18–22, 2017.
30. Cox, A. N. ed. Allen's Astrophysical Quantities. Springer, 2015, p. 244.